Bioresource Technology 253 (2018) 112–120

Contents lists available at ScienceDirect

Bioresource Technology

journal homepage: www.elsevier.com/locate/biortech

Pathway and mechanism of nitrogen transformation during composting: Functional enzymes and genes under different concentrations of PVP-AgNPs

Guangming Zeng[a,b,*], Lihua Zhang[a,b], Haoran Dong[a,b], Yaoning Chen[a,b], Jiachao Zhang[c], Yuan Zhu[a,b], Yujie Yuan[a,b], Yankai Xie[a,b], Wei Fang[a,b]

[a] College of Environmental Science and Engineering, Hunan University, Changsha 410082, PR China
[b] Key Laboratory of Environmental Biology and Pollution Control, Hunan University, Ministry of Education, Changsha 410082, PR China
[c] College of Resources and Environment, Hunan Agricultural University, Changsha 410128, PR China

GRAPHICAL ABSTRACT

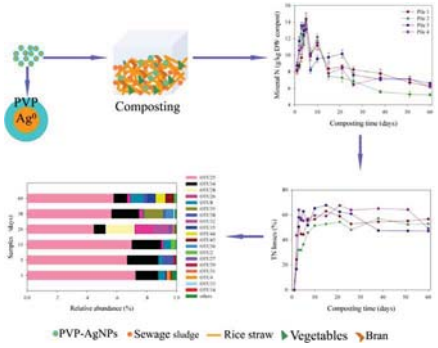

ARTICLE INFO

Keywords:
PVP-AgNPs
Composting
Nitrogen transformation
Functional enzymes
Functional genes

ABSTRACT

Polyvinylpyrrolidone coated silver nanoparticles (PVP-AgNPs) were applied at different concentrations to reduce total nitrogen (TN) losses and the mechanisms of nitrogen bio-transformation were investigated in terms of the nitrogen functional enzymes and genes. Results showed that mineral N in pile 3 which was treated with AgNPs at a concentration of 10 mg/kg compost was the highest (6.58 g/kg dry weight (DW) compost) and the TN loss (47.07%) was the lowest at the end of composting. Correlation analysis indicated that TN loss was significantly correlated with *amoA* abundance. High throughput sequencing showed that the dominant family of ammonia-oxidizing bacteria (AOB) was *Nitrosomonadaceae*, and the number of Operational Taxonomic Units (OTUs) reduced after the beginning of composting when compared with day 1. In summary, treatment with AgNPs at a concentration of 10 mg/kg compost was considerable to reduce TN losses and reserve more mineral N during composting.

1. Introduction

Sewage sludge (SS) is an essential by-product during wastewater treatment process. With the rapid expanding of wastewater treatment plants (WWTP), the production of SS also increased dramatically. Researches reported that the averagely annual production of SS in WWTP of China was 30 million tons and increased by more than 13% between 2007 and 2015 (Cai et al., 2016). SS is favorable for recycling

* Corresponding author at: College of Environmental Science and Engineering, Hunan University, Changsha 410082, PR China.
E-mail address: zgming@hnu.edu.cn (G. Zeng).

https://doi.org/10.1016/j.biortech.2017.12.095
Received 12 November 2017; Received in revised form 25 December 2017; Accepted 27 December 2017
Available online 29 December 2017

to agriculture because of considerable fractions of nitrogen, phosphorus and other fertilizing elements in it. However, SS can not be directly reused as fertilizer for the high quantities of pathogenic microbes, organic micro-pollutants and toxic heavy metals, which are strictly controlled by the legislation of SS applications (Zeng et al., 2013a). Consequently, the development of environmentally friendly and sustainable measures for disposal of SS has received much fervent attention (Vogel and Adam, 2011; Zeng et al., 2013b).

Composting is a cost-efficient and social preferred approach for solid waste management. During SS composting, unstable and complex organic matters are degraded into stable and humus-like substances without toxic effects and the composted SS is preferred as soil conditioner and organic fertilizer for agriculture (Huang et al., 2008; Tang et al., 2008). As a critical factor for evaluating the quality of final composts, nitrogen bio-transformation during SS composting is complex, including volatilization, mineralization, immobilization, nitrification and denitrification, and the loss of nitrogen is mainly caused by the release of NH_3, N_2O, N_2 and NO_x (Zhang et al., 2017). Many researchers have been exploring more effective methods to reduce nitrogen loss during SS composting. Since the high concentration of nitrogen and low C/N ratio would lead to excessive ammonia volatilization (Malińska et al., 2014; Yang et al., 2010), extra carbon sources (e.g. sawdust, straw, paper, biochar) were introduced to improve the physico-chemical properties of composting materials (Malińska et al., 2014). Other additives like lime and zeolite were also applied to alleviate the acidic pH and reduce the release of NH_3 and N_2O (Cheng et al., 2016).

The development of nanotechnology has brought huge increases in production and use of engineered nanoparticles (ENPs) (Xu et al., 2012). The project of Emerging Nanotechnologies at the Woodrow Wilson International Center for Scholars reported that consumer products containing ENPs increased by 521% between 2006 and 2011 (Feng et al., 2010; Gong et al., 2009; Impellitteri et al., 2013). Due to the antimicrobial properties, silver nanoparticles (AgNPs) are applied to various consumer products, such as food containers, sporting goods, clothing, softeners and detergents (Kim et al., 2010). Many researches have tried to illustrate the relationships between AgNPs and microorganisms. In soil ecosystem, several studies suggested that denitrifying bacteria and denitrification were easily vulnerable to AgNPs (Mishra and Singh, 2015). It was found that NO_3^--N reduction was retarded even by low concentration of AgNPs in sequencing batch reactors, and NO_2^--N kept the same low levels and this might be due to that AgNPs inhibited the activity of nitrate reductase, while brought less adverse effects on nitrite reductase under low level (Hu et al., 2011; Zhang et al., 2016c). Previous literatures reported that nitrifying bacterial activity was decreased by 86% under 1 mg/L AgNPs (Choi and Hu, 2008; Zhang et al., 2007), while other studies found that nitrification was decreased by 41.4% at the same concentration of AgNPs in an activated sludge treatment system (Fan et al., 2008; Liang et al., 2010). These previous studies provided deep insights into the impacts of AgNPs on nitrogen cycling and the related microorganisms. However, few researches linked the nitrogen transformation with the functional enzymes and genes simultaneously during composting with the existence of PVP-AgNPs and few researches studied the diversity of the functional genes which shown significant correlation with total nitrogen (TN) losses.

The present study was conducted to investigate the impacts of PVP-AgNPs under different concentrations on nitrogen bio-transformation during composting. The changes of functional enzymes activities and genes abundances for nitrogen bio-transformation were determined, since these data help explain the nitrogen changes. Also, the bacterial *amoA* gene which was significantly correlated with TN losses was sequenced to study the diversity of ammonia-oxidizing bacteria (AOB). This research represents the few researches which reveal the impacts of AgNPs on nitrogen transformation by integrating the analyses of enzyme activities and molecular level of nitrogen cycling microbial communities.

2. Experimental section

2.1. PVP-AgNPs synthesis and characterizations

Polyvinylpyrrolidone coated AgNPs (PVP-AgNPs) was chosen since this kind of AgNPs can maintain colloidal stability in composting systems where the environment is complex and the ionic strength is high with high valence background electrolytes (Gitipour et al., 2013). Briefly, 5×10^{-3} M $AgNO_3$ was dropwise (~1 drop per second) added into a vigorously stirring solution of 1% PVP and 2.5×10^{-3} M $NaBH_4$ at a volume ratio of 1:3 and this procedure was conducted in a condition of ice bath. In addition, the synthesized PVP-AgNPs were purified three times using 1 kDa dialysis membranes to clear the rest of reactants. This purification method could prevent the solutions drying, aggregating or oxidizing, and the concentration of AgNPs was kept the same by replacing the excess by-products with water.

UV–vis absorption spectrum analysis was performed using a Shimadzu UV-2550 (Japan) at a wavelength range of 300–800 nm to confirm the successful synthesis of AgNPs. Transmission electron microscopy (TEM) and energy dispersive X-ray spectrophotometer (EDX) analysis were carried out to investigate the morphology and further confirm the formation of AgNPs. Samples for TEM and EDX were prepared by adding a drop of AgNPs solution on a carbon coated copper grid and then air-dried at room temperature. The TEM and EDX photographs were captured by JEOL, JEM-2100F complemented with EDX and the accelerating voltage was 200 kV. Hydrodynamic diameter (HDD) were determined using Zetasizer Nanoseries (Malvern Instruments, UK) according to the theory of dynamic light scattering (DLS) with a 633 nm laser source and a 173° detection angle and the detection range was from 1 nm to 10 μm.

2.2. Materials preparation, composting and sampling

Sewage sludge was obtained from Yuelu wastewater plant of Changsha, China and then it was air-dried and sieved through the 100-mesh screen. Rice straw, collected from suburb of Changsha, China, was also air-dried and cut into 10 ~ 20 mm lengths. It is a kind of typical agricultural waste difficult to degrade. As the easily degradable materials to assist the composting processes, vegetables were chopped into 10–20 mm lengths after being air-dried. To improve the initial carbon to nitrogen (C/N) ratio, bran was air-dried and added into the composting piles. The characteristics of the raw materials were presented in Table 1. Initial moisture content was regulated to 65% and C/N ratio was adjusted to about 25 (Gitipour et al., 2013; Huang et al., 2017a) by blending sewage sludge, rice straw, vegetables and bran at a weight ratio of 22:36:5:5. Five indoor composting piles were set up including pile 1 (without AgNPs) and pile 2–5 which were treated with AgNPs at concentrations of 2, 10, 20, 30 mg/kg compost, respectively. The composting processes lasted for 60 days during which most of complex organic matters were degraded to stable substances. The piles were turned daily during the first 14 days and weekly afterwards. Solid samples were collected from three different locations of the piles and

Table 1
The physico-chemical characteristics of the raw materials (dry weight).

Materials	Moisture content (%)	TOC (g/kg)	TN (g/kg)	C/N ratio	pH
Rice straw	10.35	488.9	10.3	47.5	–[a]
Sewage sludge	9.48	178.9	24.2	7.4	6.74
Bran	14.62	528.2	25.1	21.0	–[a]
Vegetables	94.84	446.4	19.6	22.8	–[a]

–[a] not determined.
TOC, total organic carbon.
TN, total nitrogen.
C/N, TOC/TN.

homogenized before stored at 4 °C for determinations of physico-chemical parameters and −20 °C for DNA extraction.

2.3. Physico-chemical parameters and nitrogen functional enzymes determination

Temperature was recorded from five different positions of the composting piles using a thermometer. The NH_4^+-N, NO_3^--N, NO_2^--N concentrations were determined according to the methods in previous studies (Zhang et al., 2017) by shaking the samples in 2 M of KCl solution at a ratio of 1:50 (w/v) for 1 h to extract the mineral N. Mineral N equaled to the sum of NH_4^+-N and NO_3^--N. Samples for TN determination were ground after being dried at 105 °C for 24 h and analyzed using Kjeldahl digestion analysis. The TN losses were calculated according to the following formula (Zhang et al., 2017):

$$\text{TN loss}(\%) = 100-100[(X_1N_n)/(X_nN_1)] \quad (1)$$

in which N_1 and N_n represented the total nitrogen concentration on initial and each corresponding day, and X_1 and X_n represented ash content on initial and each corresponding day, respectively. The activities of nitrate reductase (NR), nitrite reductase (NIR), ammonia monooxygenase (AMO) and nitrite oxidoreductase (NOR) were measured referring to previous literatures (Zheng et al., 2011) (see Supplementary materials).

2.4. DNA extraction

The total genomic DNA was extracted from 0.3 g samples of each composting pile using the E.Z.N.A. ® Soil DNA Kit (OMEGA Bio-Tek, Inc., Norcross, GA, USA). The extraction was conducted according to the manufacturer's instructions. The quality and concentration of DNA extraction were determined using a NanoDrop (Thermo Scientific, Wilmington, DE, USA). The purification of crude DNA was performed using the Universal DNA Purification Kit (TIANGEN, China) according to the manufacturer's instructions for use. Three parallel extractions were performed for each compost sample.

2.5. Quantification of nitrogen functional genes

The abundances of functional genes, encoding the key enzymes involved in nitrification (*amoA* and *nxrA* encoding ammonia monooxygenase and nitrite oxidoreductase, respectively) and denitrification (*narG*, *nirK*, *nirS*, and *nosZ* encoding the membrane-bound nitrate reductase, copper-containing nitrite reductase, cd_1-containing nitrite reductase, and nitrous oxide reductase, respectively), were used to represent the abundances of functional microbes (Zhi and Ji, 2014). The quantitative PCR (qPCR) was conducted on an iCycler IQ5 Thermocycler (Bio-Rad, USA) in a system of 10 μL of 2 × SuperRedal PreMix Plus (with SYBR Green I), 0.4 μL of each primer (50 μM), 1 μL of template DNA, and 8.2 μL of sterile ultrapure water (see Supplementary materials). All the qPCR reactions set up the negative control by replacing the unknown DNA sample with sterile ultrapure water, and three parallel qPCR analyses were performed for each sample. The gene copies obtained from qPCR reaction were converted to copies per gram of dry weight (DW) compost.

2.6. High throughput sequencing and sequence analysis

Compost samples were sent to Shanghai Majorbio Bio-pharm Technology Co., Ltd. (Shanghai, China) for sequencing of bacterial functional gene *amoA* (see Supplementary materials). The raw sequences were submitted to NCBI with BioProject ID PRJNA385265.

2.7. Statistical analyses

All analyses of parameters apart from temperature which was determined from five different positions of the composting piles were performed in triplicate. For the evaluation of differences between composts from different piles, least significance difference (LSD) test was conducted at 95% confidence level using SPSS 19.0. If $P > .05$, the difference between piles was thought to be statistically insignificant. Pearson correlations coefficients were calculated using MATLAB R2013a to assess the relationships between TN losses and the functional genes of N transformation, and a correlation matrix (7 × 7) was created.

3. Result and discussion

3.1. PVP-AgNPs characterizations

The absorption peak around 400 nm suggested the formation of AgNPs, and no peaks else were found < 390 nm indicating that there were not impurities (e.g. Ag^+) in the AgNPs solution (see Supplementary materials). Spherical particles were found distributed evenly on the carbon coated copper grid and the average size was about 6 nm. And the EDX analysis diagram further suggested that the particles in TEM graph were the PVP-coated AgNPs. The average HDD of the synthesized PVP-AgNPs was about 8.5 nm. The little bit of difference between TEM size and HDD size once be reported that it might be caused by the following: (1) the process of drying TEM samples might lead to the shrinkage of the PVP molecule; (2) the aggregated PVP-AgNPs were not dispersed fully during sonication and resulted in larger HDD size; and (3) the PVP coated more than one AgNPs at the same time (El Badawy et al., 2010).

3.2. Temperatures of composting piles

As well known, temperature was an essential parameter to evaluate the performance of decomposition of organic matter during composting process (Huang et al., 2017a; Wang et al., 2013). Since the highest temperature in pile 5 was lower than 50 °C, all other parameters of pile 5 were not presented in this literature. The time courses of temperatures in other four composting piles were similar to many patterns which included three typical phases (mesophilic, thermophilic and cooling stage) (see Supplementary materials). The significant differences ($P < .05$) between all treatments were observed during the first 12 days and this was mainly caused by the population succession of mesophilic-thermophilic microorganisms. The temperatures rose dramatically during the early phases of composting due to the decomposition of easily degradable organic matter by microbes, and reached to the highest on day 5 for pile 1 (59.6 °C), day 7 for pile 2 (55.8 °C) and pile 3 (60.4 °C), and day 4 for pile 4 (61 °C), respectively. It was fastest to achieve highest temperature in pile 4 and the thermophilic phase of pile 4 lasted for 11 days, while 10 days in other piles. The temperatures over 50 °C were continued for more than 5 days, which was the requirement of Chinese National Standard and the 3-days duration of temperatures over 55 °C in all composting piles met the minimum requirement for destroying all pathogens (Zhang et al., 2011). In terms of temperature, the main impacts of AgNPs were the time when the highest temperatures reached and the values of the highest temperatures, and all treatments presented different levels of temperatures during thermophilic phase. This suggested that AgNPs might have some impacts on heterotrophic microorganisms, even promote the activities of heterotrophic microorganisms.

3.3. Nitrogen transformations

Nitrification and denitrification are two critical pathways of nitrogen transformation. The fluctuation of NH_4^+-N in composts was an important implication for the nitrogen transformations and NH_3 release (Jiang et al., 2015). In this study, NH_4^+-N dominated the inorganic nitrogen during composting, and the concentrations of NH_4^+-N in all

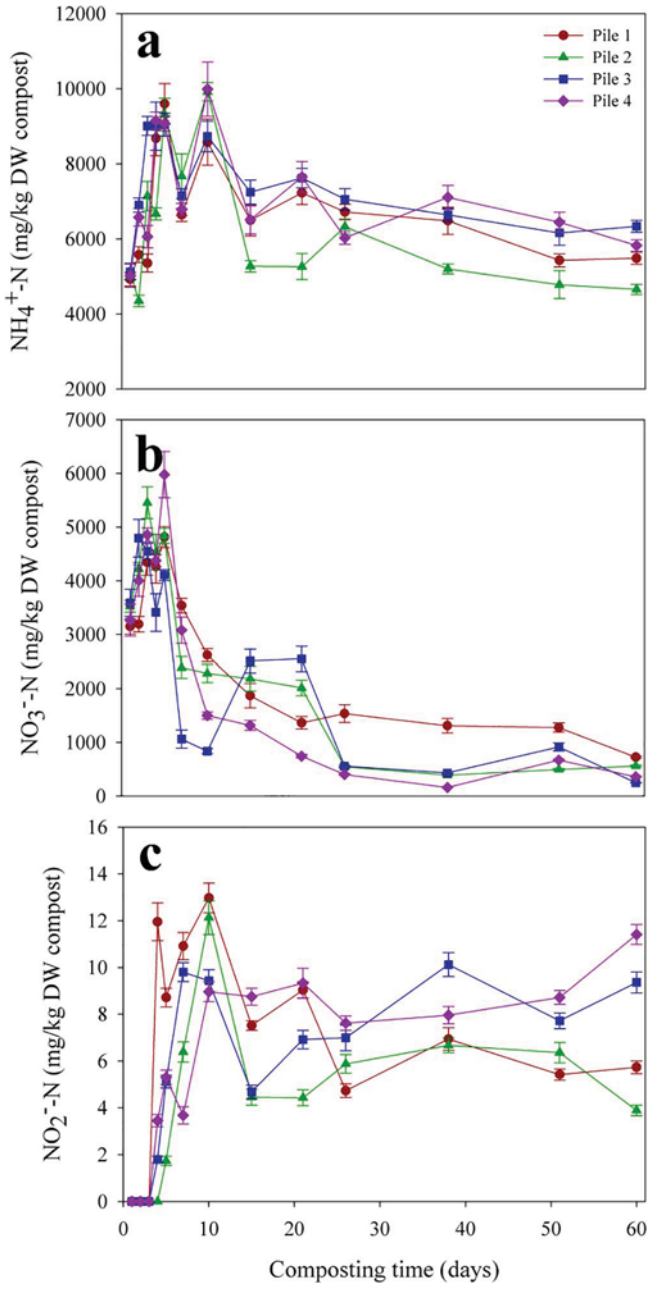

Fig. 1. Changes of (a) NH_4^+-N concentration; (b) NO_3^--N concentration and (c) NO_2^--N concentration during composting processes. Mean values and standard deviations (n = 3) were shown.

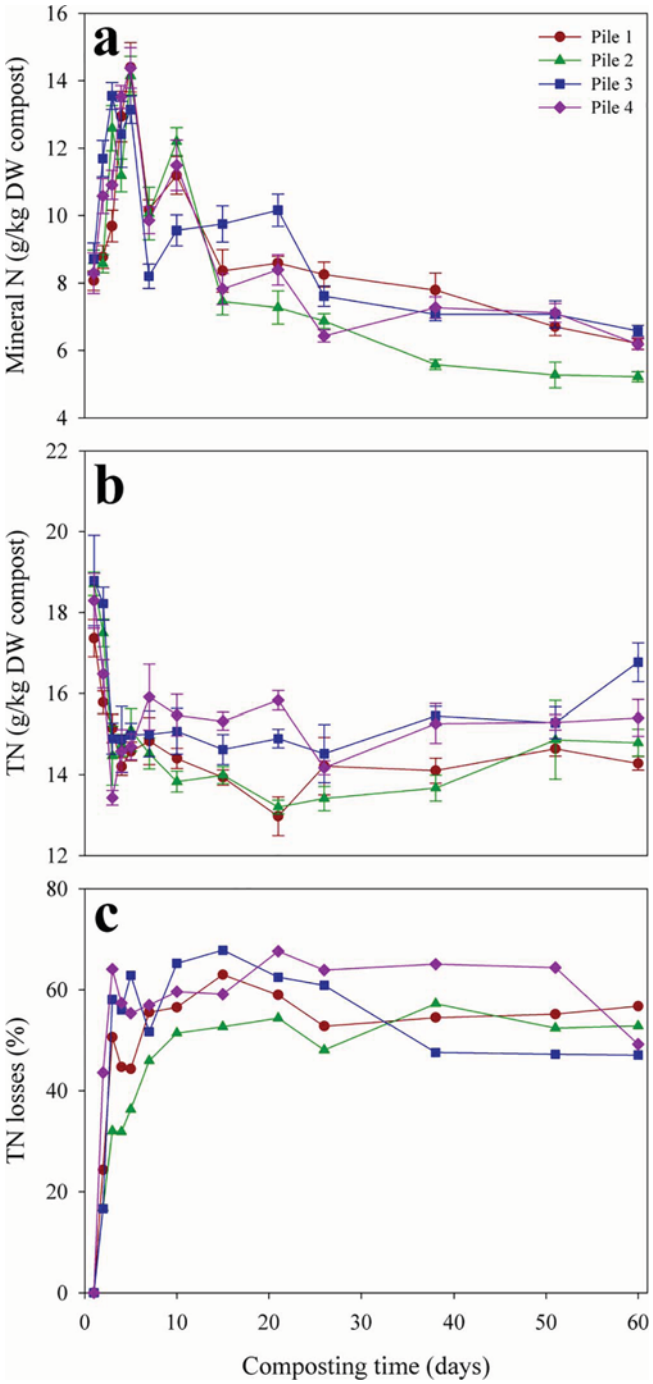

Fig. 2. Changes of (a) mineral N, (b) TN concentration, and (c) TN losses during composting processes. Mean values and standard deviations (n = 3) are presented.

treatments increased dramatically during early stages of composting because of ammonification, and reached peak value on day 5 in pile 1 and pile 3, and on day 10 in pile 2 and pile 4, respectively (Fig. 1a), this trend was similar to other literatures (Wang et al., 2013).The maximum NH_4^+-N concentration was detected in pile 4 (9990.04 mg/kg dry weight (DW) compost) into which the highest concentration of AgNPs (20 mg/kg compost) was added. The delayed peak time and greater peak value of NH_4^+-N in pile 4 might be due to that the addition of AgNPs at a concentration of 20 mg/kg compost slowed down the mineralization of organic nitrogen and inhibited transformation of NH_4^+-N to NO_2^--N during early stage of composting. Then, NH_4^+-N concentrations in all treatments decreased rapidly till day 15, which might be due to the facts that high temperature and pH provided favorable conditions for NH_3 emission, and immobilization by nitrogen fixing microbes (Wang et al., 2016b). Thereafter, it continually decreased slowly till the end of composting. The NH_4^+-N concentrations of pile 1, pile 2, pile 3 and pile 4 were 5482.44, 4655.25, 6334.96 and 5822.52 mg/kg DW compost at the end of composting, respectively. It was 1.09 ~ 1.36 times higher in pile 3 than other piles. One-way analysis of variance (ANOVA) presented a significant difference among the four treatments (F = 64.9, P < .01), and LSD tests indicated highly significant differences between pile 3 and other piles (P < .05) at the end of composting.

Similar to NH_4^+-N, NO_3^--N contents increased rapidly during the first several days of composting (Fig. 1b) owing to alkaline pH (see Supplementary materials) which provided favorable conditions for transformation of NO_2^--N to NO_3^--N by nitrite oxidizing bacteria (NOB) (Zhang et al., 2016b). The NO_3^--N in pile 3 peaked fastest to

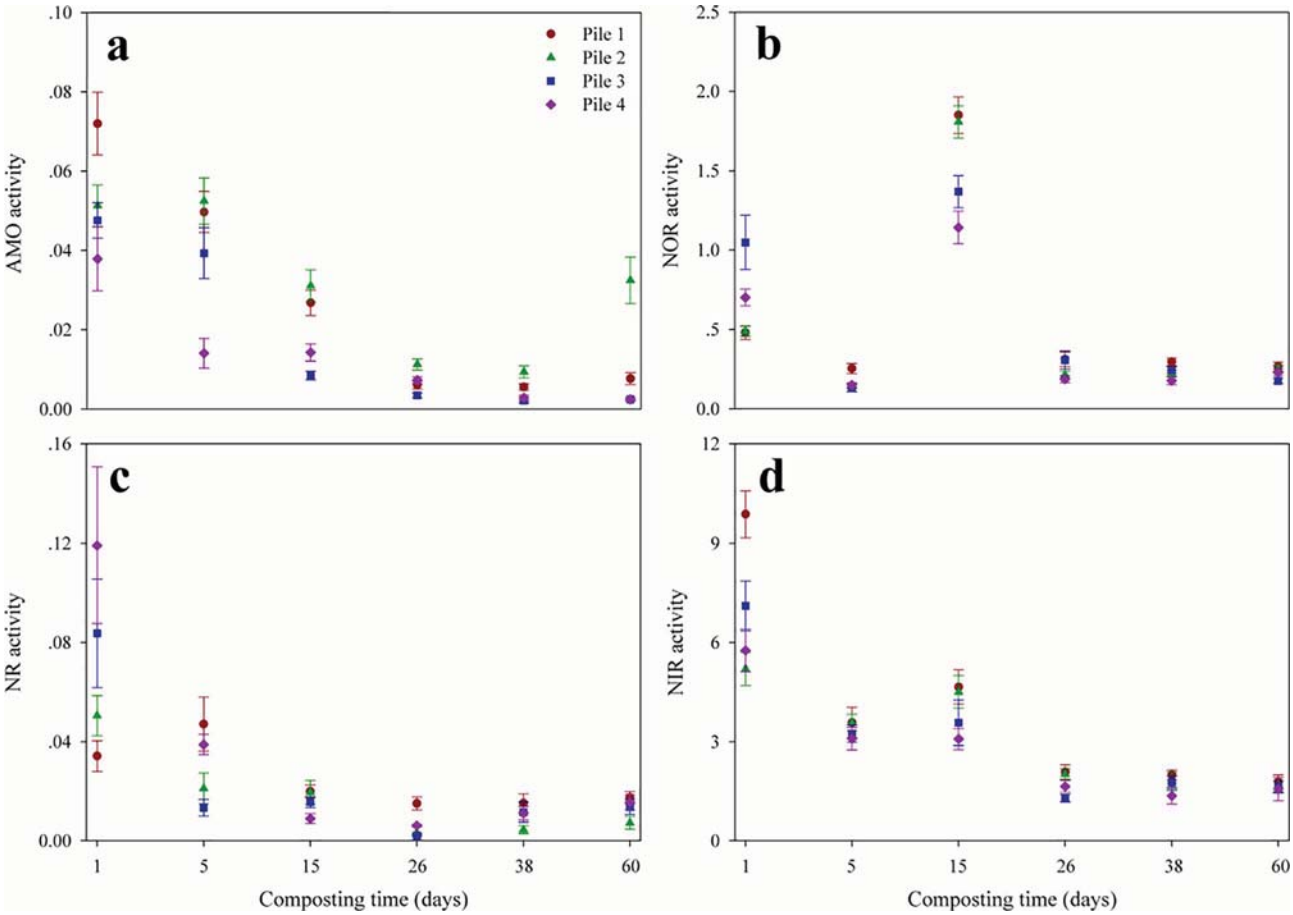

Fig. 3. Activities of functional enzymes during composting processes. The unit of activities is μmol nitrite/(min·mg protein). (a) AMO; (b) NOR; (c) NR; (d) NIR. Mean values and standard deviations (n = 3) were shown.

4791.34 mg/kg DW compost, while the peak value of NO_3^--N in pile 4 (5976.68 mg/kg DW compost) was the highest ($P < .05$). Then NO_3^--N concentrations presented downtrends, and pile 3 showed significant lower NO_3^--N content at the end of composting. According the previous study (Bustamantea et al., 2008), the exposure of unavailable NH_4^+-N to microbes could suppress the nitrification and lead to lower NO_3^--N.

As shown in Fig. 1c, the content of NO_2^--N was relatively low as it was the intermediate product generated during nitrification by ammonia-oxidizing microbes. During the first three days, NO_2^--N were not detected in all piles and increased rapidly since day 4 to peak values on day 10, then presented short periods of decline. Thereafter, the trends of NO_2^--N were divided into two groups: pile 1 and pile 2 continually decreased till the end, while pile 3 and pile 4 increased slowly. This suggested that higher concentrations of AgNPs would inhibit conversions of NO_2^--N to NO_3^--N.

The time courses of total mineral nitrogen (Fig. 2a) were similar to NH_4^+-N, mainly because that NH_4^+-N dominated the mineral nitrogen. At the beginning, mineral nitrogen contents increased dramatically though the TN declined (Fig. 2b). This might be on account of the transformation of organic nitrogen to mineral nitrogen and losses of nitrogen as NH_3, N_2O, NO_X, etc. during this process. Afterwards, concentrations of mineral nitrogen in all treatments decreased till the end of composting. With organic nitrogen was mineralized, the activities of microorganisms were thought to be increased, which induced fierce competitions for nitrogen substrates and the consequent immobilization of mineral nitrogen (Azeez and Averbeke, 2010). The mineral nitrogen concentrations were 6.2, 5.22, 6.58, and 6.18 g/kg DW compost in pile 1 ~ pile 4 in the end, respectively. The highest mineral nitrogen content was detected in pile 3 and the loss of TN in pile 3 was the lowest ($P < .05$) (Fig. 2c) at the end of composting. Comparing with the initial TN, the lowest TN loss in pile 3 was 13.76% which was lower than the control pile (17.74%) by 22.4%. While in the previous study, the lowest nitrogen loss (19.72%) was detected in the pile which was treated with 10% biochar and 10% zeolite during pig manure composting (Wang et al., 2017). Therefore, the impact on the conservations of nitrogen and improvements of N availability was the most remarkable when pile was treated with AgNPs of 10 mg/kg compost in this study.

3.4. Activities of key enzymes

Biological transformation of nitrogen is critically dependent on the activities of key enzymes. Many previous literatures reported that nitrification and denitrification are two key pathways in nitrogen biotransformation (Zheng et al., 2011). AMO and NOR are two key enzymes for nitrification, whereas NR and NIR are crucial to denitrification (Zheng et al., 2011). As shown in Fig. 3a, the activity of AMO in pile 3 was the lowest since day 15, indicating that the existence of AgNPs at a concentration of 10 mg/kg compost inhibited the activity of AMO. It was significantly lower than pile 2 during the whole composting but was insignificantly lower than pile 1 and pile 4 after day 26. The presence of AgNPs at a concentration of 2 mg/kg compost stimulated the activity of AMO. These observations further explained the higher NH_4^+-N in pile 3 at the end of composting (Fig. 1a). Fig. 4b showed that the addition of AgNPs at a concentration of 20 mg/kg compost inhibited the activity of NOR which was significantly higher in pile 1 than pile 4, while insignificantly higher than pile 2 and pile 3.

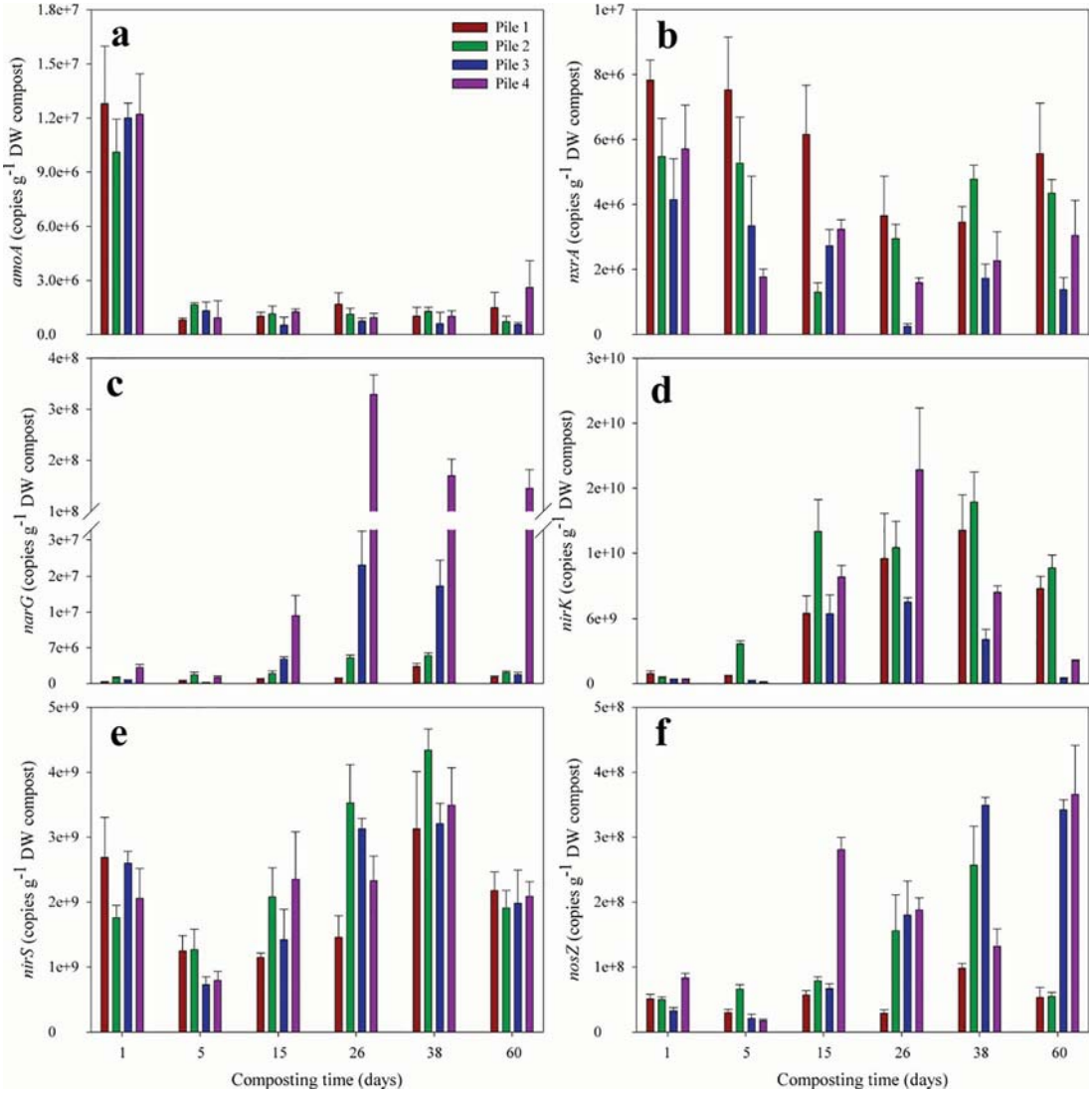

Fig. 4. Changes of functional genes copy numbers during composting processes. Mean values and standard deviations (n = 3) were shown.

These observations were consistent with the higher concentrations of NO_3^--N in pile 1 since the day 26 of composting processes (Fig. 1b). However the highest activity of AMO in pile 2 did not result in higher concentration of NO_2^--N (Fig. 1c), and this might be due to the relatively higher activities of NOR and NIR (Fig. 3) than pile 3 and pile 4, and lower activity of NR. As shown in Fig. 3c and d, the activity of NR was higher in pile 1, and that of NIR were higher in pile 1 and pile 2, resulting in lower concentration of NO_2^--N in pile 1 and pile 2 during the cooling and maturation stages. It was in accordance with other literatures that found higher levels of AgNPs inhibited the activities of NR and NIR (Zhang et al., 2016c).

3.5. Quantification of nitrogen functional genes

The genes (*amoA*, *nxrA*, *narG*, *nirK*, *nirS* and *nosZ*) were quantified for all piles during composting (Fig. 4). The highest abundances of *amoA* which is the marker of aerobic oxidation of NH_4^+-N to NO_2^--N were determined at the beginning of composting in all piles and then decreased rapidly. The copy numbers of *amoA* in pile 3 were restrained by AgNPs since day 15 till the end of composting, resulting in higher concentration of NH_4^+-N in pile 3 during the same period. Among the four piles, the average copy number of *amoA* in pile 3 was the lowest and the order of other three piles was: pile 4 > pile 1 > pile 2. This indicated the vulnerability of AOB to AgNPs at a concentration of 10 mg/kg compost, while it was interesting to found that the *amoA* copies increased under a concentration of 20 mg/kg compost. Other interesting phenomena were found by previous studies that the impact on *amoA* was more pronounced in 35-nm AgNPs treated samples than 5-nm AgNPs treated samples (Yang et al., 2014). As shown in Fig. 4b, higher *nxrA* copies were detected in pile 1 during the whole composting period, which suggested that NOB was vulnerable to AgNPs and it was more sensitive in pile 3 treated with 10 mg/kg compost AgNPs. The order of average *nxrA* abundances in four piles was pile 1 > pile 2 > pile 4 > pile 3. The similar temporal variation trends of *nxrA* and *amoA* in pile 1 might be due to the similar survival conditions that both AOB and NOB needed aerobic conditions and were autotrophic, and the ecological relation that AOB supplied NO_2^--N by oxidizing NH_4^+-N to NO_2^--N for NOB to transform NO_2^--N to NO_3^--N (Zhi and Ji, 2014). However, the changes of *nxrA* were not consistent with that of *amoA* in other three piles since the disturbance of AgNPs.

The detectability of *narG*, *nirK*, *nirS*, and *nosZ* suggested the occurrence of denitrification during composting of all treatments. *NarG* is the well-known representative encoding membrane-bound nitrate reductase to perform the reduction of NO_3^--N to NO_2^--N (Lopez-Gutierrez et al., 2004). The highest abundance of *narG* of each pile was detected on day 26 or 38 and the time courses of *narG* gene in all composting piles exhibited an increase from the beginning to day 26 or 38 and then decrease till the end of composting processes (Fig. 4c).

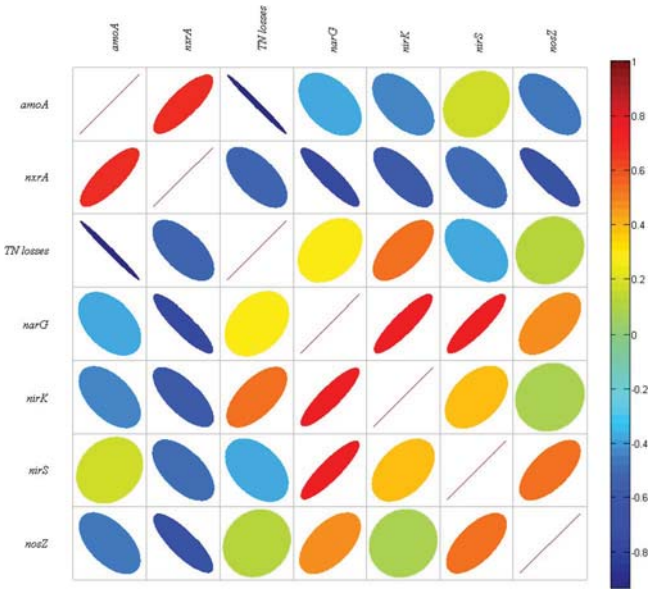

Fig. 5. Relationships between TN losses and functional genes (*amoA*, *nxrA*, *narG*, *nirK*, *nirS*, and *nosZ*) of pile 3. Warm color represents positive correlation coefficients, whereas cool color represents negative correlation coefficients, and smaller ovals represent lower correlations, while bigger ovals represent stronger correlations.

Table 2
Richness and diversity of bacterial *amoA* gene sequences in pile 3 during composting processes.

Samples	Sequences	OTUs	Chao 1	ACE	Shannon	Coverage
1	11,919	27	27	27	1.06	1
5	19,406	6	6	0	0.94	1
15	12,425	8	8	8	1.50	1
26	18,835	10	10	10	1.60	1
38	15,705	10	10	0	0.99	1
60	14,627	12	12	12	1.33	1

All values were calculated based on cutoff 3% dissimilarity.

Among the four piles, *narG* in pile 4 was the highest especially from day 26 to the end of composting ($p < .05$). The order of average *narG* abundance was pile 4 > pile 3 > pile 2 > pile 1, suggesting that AgNPs had a positive impact on *narG* gene and the impact was more pronounced under exposure of higher AgNPs concentration. This was similar to other researches that found AgNPs did not significantly influence the expression of *narG* and even could stimulate the survival of microbes (Fajardo et al., 2014; Xiu et al., 2012). *NirK* and *nirS* are two functional genes involved in the second denitrification step, namely the reduction of NO_2^--N to NO and this is the first stage for production of gas in denitrification (Huang et al., 2017b). The abundance of *nirK* in all piles increased till day 26 or 38 and then decreased till the end of composting (Fig. 4d). Order of average *nirK* copies was pile 2 > pile 1 > pile4 > pile 3 and that of *nirS* was pile 2 > pile 4 > pile 3 > pile 1. While for *nirS* gene abundance, it decreased rapidly in all piles during the first 5 days and increased continuously till day 38, and decreased again till the end (Fig. 4e). The average copy number of *nirK* was about 2–4-fold higher than that of *nirS*, similar to other studies (Wang et al., 2013). The higher *nirK* gene abundance indicated that it was more tolerant of AgNPs, and it also suggested that *nirK* was dominant in nitrite reduction step and the main contributor to generation of greenhouse gas (NO) (Wang et al., 2016a). Since both *nirK* and *nirS* participated in the second step of denitrification, the total abundances of the two genes were calculated to evaluate the potential for transformation of NO_2^--N to NO (Yan et al., 2003). The variation tendencies were similar to that of *nirK* with increasing from beginning to day 26 or 38, and then decreasing till the end of composting. The average total abundances of *nirK* and *nirS* in all piles arranged in the order of pile 2 > pile 1 > pile 4 > pile 3, which was in accordance with the single *nirK* gene and was similar with that of *narG*. This might be due to the higher *nirK* gene abundance than *nirS*, and on the other hand, *narG* codase catalyzed the transformation of NO_3^--N to NO_2^--N, providing substrate NO_2^--N for *nirK* codase and *nirS* codase to convert it into NO so that their abundances might be influenced by *narG*. *NosZ* is often regarded as the marker for the last step of denitrification in which N_2O was conversed into N_2. As shown in Fig. 4f, the abundance of *nosZ* in each pile exhibited different change tendencies. In pile 1, the highest copy number was detected on day 38 with constant fluctuations during composting process. In pile 2 and pile 3, *nosZ* abundance increased till day 38 and then decreased till the end of composting. While in pile 4, it decreased from day 1 to day 5 followed by increasing till day 15, and then decreased till day 38 which was followed by an increase till the end when the copy number was the highest. According to the comparison among the four piles, the average abundance of *nosZ* in pile 4 was highest. The order of remaining three piles were pile 3 > pile 2 > pile 1. This indicated that the stimulation to *nosZ* was more obvious with higher AgNPs.

3.6. Correlation between TN losses and nitrogen functional genes

As shown in Fig. 2c, TN losses in pile 3 were the lowest compared with other three piles. So, correlation coefficients were determined between TN losses and nitrogen functional genes in pile 3 (Fig. 5). The results of correlation analysis showed that TN loss in pile 3 was most significantly and negatively correlated with the abundance of *amoA* ($r = -0.9317$, $P < .01$). This can be interpreted as that the *amoA* gene encodes AMO to convert NH_4^+-N into NO_2^--N, which results in the decrease of NH_4^+-N. And the lower concentration of NH_4^+-N will reduce NH_3 emissions and TN losses (Zhang et al., 2011). Song et al. (2016) reported a negative correlation between NH_3 and ammonia-oxidizing archaea (AOA), but a positive relationship between NH_3 and

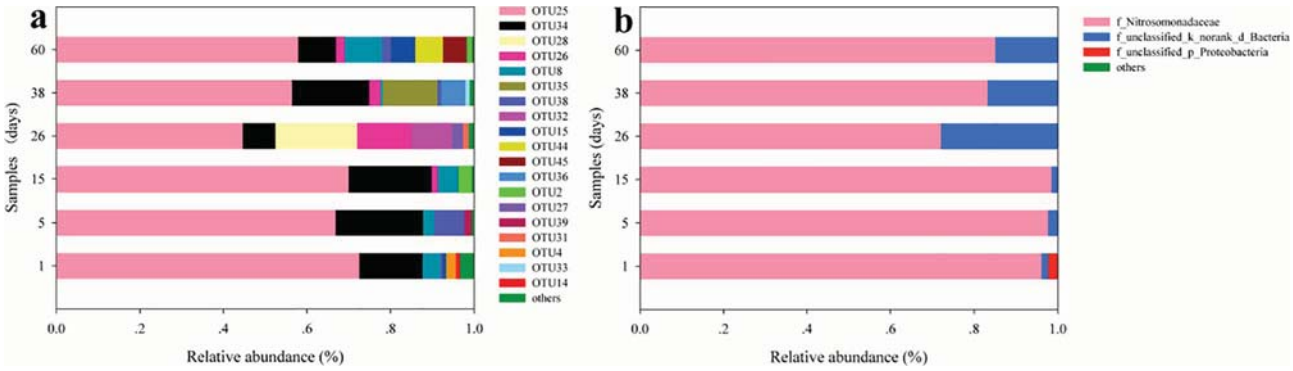

Fig. 6. Relative abundance of bacterial *amoA* gene at (a) OTUs level; (b) family level.

AOB. Additionally, both AOA and AOB may be inhibited under high concentrations of NH_3 (Jung et al., 2014).

3.7. Diversity of ammonia-oxidizing bacteria (AOB)

According to the result of the correlation analysis between TN losses and functional genes in pile 3, the diversity of *amoA* gene in pile 3 was studied by sequencing. Totally, 92,917 sequences of bacterial *amoA* with sequences of 11,919, 19,406, 12,425, 18,835, 15,705, and 14,627 for each sample respectively, were obtained after removal of low quality sequences (< 20), sequences smaller than 50 bp, primer chimeras, non-ribosomal sequences and sequence tags (Table 2). The average length of sequences was about 469 bp. All sequences were clustered into 45 OTUs in total. Highest number of OTUs was detected in samples from day 1 (27 OTUs), while the lowest number was 6 which was observed in samples from day 5 (6 OTUs), and then it increased continuously to 12 OTUs at the end of composting. The calculation of Chao1 and ACE which were the indices of community richness revealed that AOB species were the richest at the beginning of composting. Also, the Shannon index of AOB in each sample suggested that the diversity of AOB from day 1 was the highest, while it was lowest in samples from day 5. Both the richness and diversity of AOB community began to increase from day 5, which was similar to other studies that only found some weak denaturing gradient gel electrophoresis (DGGE) bands during thermophilic phase of agricultural composting (Zhang et al., 2016a).

Fig. 6 revealed the relative abundances of phylotypes at OTUs and family level in each sample from pile 3 during composting. Fig. 6a showed that OTU 25 (44.61–72.561%), OTU 34 (7.84–20.91%) and OTU 8 (0.04–8.96%) existed during the entire composting process, and OTU 25 dominated AOB community with slight reduces during composting process. Also, OTU 34 played an important role during the ammoxidation process. However, some kinds of OTUs (OTUs 14 and OTUs 4) which existed at the beginning of composting disappeared under the exposure to AgNPs. As shown in Fig. 6b, the predominant family *Nitrosomonadaceae* which was affiliated to *Proteobacteria* and *β-Proteobacteria* at phylum and class level respectively ranged from 71.63% to 98.44% in all samples in terms of relative abundance. Previous studies also reported that *Proteobacteria* was the most predominant phylum counting for about 7.4%～46.4% of total effective sequences in twelve wastewater treatments systems (Shu et al., 2016). It was once detected that *Proteobacteria* was the largest group which could resist silver nanoparticles (Yang et al., 2014), this was in accordance with the present literature. Lai et al. (2014) found that *β-Proteobacteria* was the absolutely predominant class with relative abundance of more than 90%, while the abundance of *α-Proteobacteria* was < 7% when about 10 mg/L NO_3^--N was added into membrane biofilm reactor in their study. The family of *Nitrosomonadaceae* could be further divided into *Nitrosomonas*, *Nitrosospira* and some unclassified genuses. It was once reported that *Nitrosomonas* was the predominant AOB, while the abundance of *Nitrosospira* was relatively low in the landfill leachate treatment system under high organic load (Remmas et al., 2016). On the other hand, the genus *Nitrosomonas* detected in the present study was related to *Nitrosomonas sp*. Nm 84, *Nitrosomonas sp*. Is 79A3, *Nitrosomonas eutropha* and some unclassified species with 97% similarity at least. As for *Nitrosospira*, it was closely associated with *Nitrosospira briensis*, which has also been suggested that *Nitrosospira briensis* was the representative belonging to *Nitrosospira* genus that was previously found in land leachate treatment plants (Urakawa et al., 2015; Yapsakli et al., 2011). However, the species of *Nitrosomonas sp*. Is 79A3, *Nitrosomonas eutropha* and *Nitrosospira briensis* were undetectable since day 5 of the composting process, which indicated that these three AOB species were easily vulnerable to AgNPs at concentration of 10 mg/kg compost. The results of unweighted PCoA analysis on species level reveled that most of samples possessed different species (see Supplementary materials). Samples of day 5, 15, 26, 38 were grouped together with high similarity between day 5 and 38, while samples of day 1 and day 60 showed quite different species compared with other samples.

4. Conclusion

In summary, the results of the present study showed that concentration of mineral N was the highest and the TN loss was the lowest at the end of composting when treating compost with AgNPs at a concentration of 10 mg/kg compost. The results also revealed that AgNPs brought different impacts on functional enzymes and genes for nitrogen bio-transformation. These results provided a deeper insight into the bio-transformation of nitrogen and a new method to reduce TN losses.

Acknowledgements

This study was financially supported by the National Natural Science Foundation of China (51521006, 51378190, 51409100, 51408219) and the Program for Changjiang Scholars and Innovative Research Team in University (IRT-13R17).

Appendix A. Supplementary data

Supplementary data associated with this article can be found, in the online version, at http://dx.doi.org/10.1016/j.biortech.2017.12.095.

References

Azeez, J.O., Averbeke, W.V., 2010. Nitrogen mineralization potential of three animal manures applied on a sandy clay loam soil. Bioresource Technol. 101, 5645–5651.
Bustamantea, M.A., Paredesa, C., Marhuenda-Egeab, F.C., Pérez-Espinosaa, A., Bernalc, M.P., Morala, R., 2008. Co-composting of distillery wastes with animal manures: carbon and nitrogen transformations in the evaluation of compost stability. Chemosphere 72, 551–557.
Cai, L., Chen, T.B., Gao, D., Yu, J., 2016. Bacterial communities and their association with the bio-drying of sewage sludge. Water Res. 90, 44–51.
Cheng, Y., He, H.J., Yang, C.P., Zeng, G.M., Li, X., Chen, H., Yu, G.L., 2016. Challenges and solutions for biofiltration of hydrophobic volatile organic compounds. Biotechnol. Adv. 34, 1091–1102.
Choi, O., Hu, Z., 2008. Size dependent and reactive oxygen species related nanosilver toxicity to nitrifying bacteria. Environ. Sci. Technol. 42, 4583–4588.
El Badawy, A.M., Luxton, T.P., Silva, R.G., Scheckel, K.G., Suidan, M.T., Tolaymat, T.M., 2010. Impact of environmental conditions (pH, ionic strength, and electrolyte type) on the surface charge and aggregation of silver nanoparticles suspensions. Environ. Sci. Technol. 44, 1260–1266.
Fajardo, C., Saccà, M.L., Costa, G., Nande, M., Martin, M., 2014. Impact of Ag and Al_2O_3 nanoparticles on soil organisms: In vitro and soil experiments. Sci. Total Environ. 473–474, 254–261.
Fan, T., Liu, Y.G., Feng, B.Y., Zeng, G.M., Yang, C.P., Zhou, M., Zhou, H.Z., Tan, Z.F., Wang, X., 2008. Biosorption of cadmium (II), zinc (II) and lead (II) by *Penicillium simplicissimum*: Isotherms, kinetics and thermodynamics. J. Hazard Mater. 160, 655–661.
Feng, Y., Gong, J.L., Zeng, G.M., Niu, Q.Y., Zhang, H.Y., Niu, C.G., Deng, J.H., Yan, M., 2010. Adsorption of Cd (II) and Zn (II) from aqueous solutions using magnetic hydroxyapatite nanoparticles as adsorbents. Chem. Eng. J. 162, 487–494.
Gitipour, A., Badawy, A.E., Arambewela, M., Miller, B., Scheckel, K., Elk, M., Ryu, H., Gomez-Alvarez, V., Domingo, J.S., Thiel, S., 2013. The impact of silver nanoparticles on the composting of municipal solid waste. Environ. Sci. Technol. 47, 14385–14393.
Gong, J.L., Wang, B., Zeng, G.M., Yang, C.P., Niu, C.G., Niu, Q.Y., Zhou, W.J., Liang, Y., 2009. Removal of cationic dyes from aqueous solution using magnetic multi-wall carbon nanotube nanocomposite as adsorbent. J. Hazard Mater. 164, 1517–1522.
Hu, X.J., Wang, J.S., Liu, Y.G., Li, X., Zeng, G.M., Bao, Z.L., Zeng, X.X., Chen, A.W., Long, F., 2011. Adsorption of chromium (VI) by ethylenediamine-modified cross-linked magnetic chitosan resin: Isotherms, kinetics and thermodynamics. J. Hazard Mater. 185, 306–314.
Huang, C., Zeng, G.M., Huang, D.L., Lai, C., Xu, P., Zhang, C., Cheng, M., Wan, J., Hu, L., Zhang, Y., 2017a. Effect of Phanerochaete chrysosporium inoculation on bacterial community and metal stabilization in lead-contaminated agricultural waste composting. Bioresource Technol. 243, 294–303.
Huang, M.L., Wang, Z., Qi, R., 2017b. Enhancement of the complete autotrophic nitrogen removal over nitrite process in a modified single-stage subsurface vertical flow constructed wetland: effect of saturated zone depth. Bioresource Technol. 233, 191–199.
Huang, D.L., Zeng, G.M., Feng, C.L., Hu, S., Jiang, X.Y., Tang, L., Su, F.F., Zhang, Y., Zeng, W., Liu, H.L., 2008. Degradation of lead-contaminated lignocellulosic waste by *Phanerochaete Chrysosporium* and the reduction of lead toxicity. Environ. Sci. Technol.

42, 4946–4951.
Impellitteri, C.A., Harmon, S., Silva, R.G., Miller, B.W., Scheckel, K.G., Luxton, T.P., Schupp, D., Panguluri, S., 2013. Transformation of silver nanoparticles in fresh, aged, and incinerated biosolids. Water Res. 47, 3878–3886.
Jiang, J.S., Liu, X.L., Huang, Y.M., Huang, H., 2015. Inoculation with nitrogen turnover bacterial agent appropriately increasing nitrogen and promoting maturity in pig manure composting. Waste Manage. 39, 78–85.
Jung, M.Y., Well, R., Min, D., Giesemann, A., Park, S.J., Kim, J.G., Kim, S.J., Rhee, S.K., 2014. Isotopic signatures of N_2O produced by ammonia-oxidizing archaea from soils. ISME J. 8, 1115–1125.
Kim, B., Park, C.S., Murayama, M., Hochella Jr., M.F., 2010. Discovery and characterization of silver sulfide nanoparticles in final sewage sludge products. Environ. Sci. Technol. 44, 7509–7514.
Lai, C.Y., Yang, X.E., Tang, Y.N., Rittmann, B.E., Zhao, H.P., 2014. Nitrate shaped the selenate-reducing microbial community in a hydrogen-based biofilm reactor. Environ. Sci. Technol. 48, 3395–3402.
Liang, Z., Das, A., Hu, Z.Q., 2010. Bacterial response to a shock load of nanosilver in an activated sludge treatment system. Water Res. 44, 5432–5438.
Lopez-Gutierrez, J.C., Henry, S., Hallet, S., Martin-Laurent, F., Catroux, G., Philippot, L., 2004. Quantification of a novel group of nitrate-reducing bacteria in the environment by real-time PCR. J. Microbiol. Methods 57, 399–407.
Malińska, K., Zabochnicka-Świątek, M., Dach, J., 2014. Effects of biochar amendment on ammonia emission during composting of sewage sludge. Ecol. Eng. 71, 474–478.
Mishra, S., Singh, H.B., 2015. Biosythesized silver nanoparticles as a nanoweapon against phytopathogens: exploring their scope and potential in agriculture. Appl. Microbiol. Biotechnol. 99, 1097–1107.
Remmas, N., Melidis, P., Katsioupi, E., Ntougias, S., 2016. Effects of high organic load on *amoA* and *nirS* gene diversity of an intermittently aerated and fed membrane bioreactor treating landfill leachate. Bioresource Technol. 220, 557–565.
Shu, D.T., He, Y.L., Yue, H., Wang, Q.Y., 2016. Metagenomic and quantitative insights into microbial communities and functional genes of nitrogen and iron cycling in twelve wastewater treatment systems. Chem. Eng. J. 290, 21–30.
Song, H., Che, Z., Cao, W.C., Huang, T., Wang, J.G., Dong, Z.R., 2016. Changing roles of ammonia-oxidizing bacteria and archaea in a continuously acidifying soil caused by over-fertilization with nitrogen. Environ. Sci. Pollut. Res. 23, 11964–11974.
Tang, L., Zeng, G.M., Shen, G.L., Li, Y.P., Zhang, Y., Huang, D.L., 2008. Rapid detection of picloram in agricultural field samples using a disposable immunomembrane-based electrochemical sensor. Environ. Sci. Technol. 42, 1207–1212.
Urakawa, H., Garcia, J.C., Nielsen, J.L., Le, V.Q., Kozlowski, J.A., Stein, L.Y., Lim, C.K., 2015. *Nitrosospira lacus* sp. Nov., a psychrotolerant, ammonia-oxidizing bacterium from sandy lake sediment. Int. J. Syst. Evol. Micr. 65, 242–250.
Vogel, C., Adam, C., 2011. Heavy metal removal from sewage sludge ash by thermochemical treatment with gaseous hydrochloric acid. Environ. Sci. Technol. 45, 7445–7450.
Wang, Q., Awasthi, M.K., Ren, X.N., Zhao, J.C., Li, R.H., Wang, Z., Chen, H.Y., Wang, M.J., Zhang, Z.Q., 2017. Comparison of biochar, zeolite and their mixture amendment for aiding organic transformation and nitrogen conservation during pig manure composting. Bioresource Technol. 245, 300–308.
Wang, H.L., Ji, G.D., Bai, X.Y., 2016a. Distribution patterns of nitrogen micro-cycle functional genes and their quantitative coupling relationships with nitrogen transformation rates in a biotrickling filter. Bioresource Technol. 209, 100–107.
Wang, Q., Wang, Z., Awasthi, M.K., Jiang, Y.H., Li, R.H., Ren, X.N., Zhao, J.C., Shen, F., Wang, M.J., Zhang, Z.Q., 2016b. Evaluation of medical stone amendment for the reduction of nitrogen loss and bioavailability of heavy metals during pig manure composting. Bioresource Technol. 220, 297–304.
Wang, C., Lu, H.H., Dong, D., Deng, H., Strong, P.J., Wang, H.L., Wu, W.X., 2013. Insight into the effects of biochar on manure composting: evidence supporting the relationship between N_2O emission and denitrifying community. Environ. Sci. Technol. 47, 7341–7349.
Xiu, Z.M., Zhang, Q.B., Puppala, H.L., Colvin, V.L., Alvarez, P.J.J., 2012. Negligible particle-specific antibacterial activity of silver nanoparticles. Nano Lett. 12, 4271–4275.
Xu, P., Zeng, G.M., Huang, D.L., Feng, C.L., Hu, S., Zhao, M.H., Lai, C., Wei, Z., Huang, C., Xie, G.X., Liu, Z.F., 2012. Use of iron oxide nanomaterials in wastewater treatment: a review. Sci. Total Environ. 424, 1–10.
Yan, T.F., Fields, M.W., Wu, L.Y., Zu, Y.G., Tiedje, J.M., Zhou, J.Z., 2003. Molecular diversity and characterization of nitrite reductase gene fragments (*nirK* and *nirS*) from nitrate- and uranium-contaminated groundwater. Environ. Microbiol. 5, 13–24.
Yang, C.P., Chen, H., Zeng, G.M., Yu, G.L., Luo, S.L., 2010. Biomass accumulation and control strategies in gas biofiltration. Biotechnol. Adv. 28, 531–540.
Yang, Y., Quensen, J., Mathieu, J., Wang, Q., Wang, J., Li, M.Y., Tiedje, J.M., Alvarez, P.J.J., 2014. Pyrosequencing reveals higher impact of silver nanoparticles than Ag^+ on the microbial community structure of activated sludge. Water Res. 48, 317–325.
Yapsakli, K., Aliyazicioglu, C., Mertoglu, B., 2011. Identification and quantitative evaluation of nitrogen-converting organisms in a full-scale leachate treatment plant. J. Environ. Manage. 92, 714–723.
Zeng, G.M., Chen, M., Zeng, Z.T., 2013a. Risks of neonicotinoid pesticides. Science 340, 1403.
Zeng, G.M., Chen, M., Zeng, Z.T., 2013b. Shale gas: surface water also at risk. Nature 499, 154.
Zhang, Z.H., Gao, P., Li, M.Q., Cheng, J.Q., Liu, W., Feng, Y.J., 2016c. Influence of silver nanoparticles on nutrient removal and microbial communities in SBR process after long-term exposure. Sci. Total Environ. 569–570, 234–243.
Zhang, J.C., Zeng, G.M., Chen, Y.N., Yu, M., Yu, Z., Li, H., Yu, Y., Huang, H.L., 2011. Effects of physico-chemical parameters on the bacterial and fungal communities during agricultural waste composting. Bioresource Technol. 102, 2950–2956.
Zhang, J.C., Luo, L., Gao, J., Peng, Q.H., Huang, H.L., Chen, A.W., Lu, L.H., Yan, B.H., Wong, J.W.C., 2016a. Ammonia-oxidizing bacterial communities and shaping factors with different *Phanerochaete chrysosporium* inoculation regimes during agricultural waste composting. RSC Adv. 6, 61473–61481.
Zhang, Y., Zhao, Y., Chen, Y.N., Lu, Q., Li, M.X., Wang, X.Q., Wei, Y.Q., Xie, X.Y., Wei, Z.M., 2016b. A regulating method for reducing nitrogen loss based on enriched ammonia-oxidizing bacteria during composting. Bioresource Technol. 221, 276–283.
Zhang, Y., Zeng, G.M., Tang, L., Huang, D.L., Jiang, X.Y., Chen, Y.N., 2007. A hydroquinone biosensor based on immobilizing laccase to modified core-shell magnetic nanoparticles supported on carbon paste electrode. Biosens. Bioelectron. 22, 2121–2126.
Zhang, L.H., Zeng, G.M., Dong, H.R., Chen, Y.N., Zhang, J.C., Yan, M., Zhu, Y., Yuan, Y.J., Xie, Y.K., Huang, Z.Z., 2017. The impact of silver nanoparticles on the co-composting of sewage sludge and agricultural waste: Evolutions of organic matter and nitrogen. Bioresource Technol. 230, 132–139.
Zheng, X., Wu, R., Chen, Y.G., 2011. Effects of ZnO nanopartilces on wastewater biological nitrogen and phosphorus removal. Environ. Sci. Technol. 45, 2826–2832.
Zhi, W., Ji, G.D., 2014. Quantitative response relationships between nitrogen transformation rates and nitrogen functional genes in a tidal flow constructed wetland under C/N ratio constraints. Water Res. 64, 32–41.